

## MICROSTRUCTURE EVOLUTION OF *IN SITU* COMPOSITE COATINGS FABRICATED BY LASER CLADDING WITH DIFFERENT POWERS

### RAZVOJ MIKROSTRUKTURE KOMPOZITNIH PREVLEK IZDELANIH Z RAZLIČNIMI ENERGIJAMI LASERSKEGA NATALJEVANJA

Youfeng Zhang\*, Guangyu Han, Shasha He, Wanwan Yang

School of Materials Engineering, Shanghai University of Engineering Science, No.333 Longteng Rd., Shanghai 201620, China

Prejem rokopisa – received: 2021-02-29; sprejem za objavo – accepted for publication: 2021-03-04

doi:10.17222/mit.2020.194

*In situ* reaction-synthesized TiB-reinforced titanium-matrix composite coatings were fabricated using the rapid, non-equilibrium synthesis technique of laser cladding. The Ti and B mixture was the original powders, while the Ti-matrix composite coatings enhanced with TiB were treated on a Ti-6Al-4V surface with different laser scan powers of 2.5 kW, 3.0 kW and 3.5 kW. The phase composition, microstructure evaluation, and microhardness of the cladding coatings were investigated by X-ray diffractometry (XRD), scanning electron microscopy (SEM) and microhardness. The composite coatings mainly consist of black fishbone-shaped  $\alpha$ -Ti dendrites and white needle-like TiB phases. The microstructure evolution from the top to the bottom of the coatings was investigated. The TiB reinforcement dispersed homogeneously in the composite coatings and a fine microstructure was obtained in a sample fabricated with a laser power of 3.0 kW. The microhardness of the cladding coatings fabricated by different powers was over 2-fold greater than that of the Ti-6Al-4V titanium alloy substrate and achieved a maximum average of 792.2 HV with the laser power of 3.0 kW. The microstructures and properties of the coatings were changed by adjusting of the laser cladding power. The effects of the laser scan power on the microstructure, hardness and friction and wear properties of the laser cladding coatings were investigated and discussed.

Keywords: Laser cladding; Ti-6Al-4V alloy; Laser scanning power; Microstructure evolution; Composite coatings

Avtorji pričujočega članka so z *in situ* reakcijsko sintezo izdelali prevleke kompozitov na osnovi Ti, ojačanih s titanovim boridom (TiB). Kompozite so izdelali s pomočjo sinteze hitrega neravnotežnega laserskega pretaljevanja. Površino zlitine Ti-6Al-4V, na kateri je bila nanešena mešanica originalnega Ti in B prahu, so skenirali oziroma pretaljevali z laserjem različnih moči (2,5 kW, 3,0 kW in 3,5 kW). Izdelane prevleke so po hitrem strjevanju in ohlajanju okarakterizirali z rentgensko difrakcijo (XRD), vrstičnim elektronskim mikroskopom (SEM) in merilnikom mikrotrdot. Kompozitne prevleke so bile v glavnem sestavljene iz  $\alpha$ -Ti dendritov s strukturo ribjih kosti in bele igličaste faze TiB. Ugotavljali so, kako je potekal razvoj mikrostruktur od površine do spodnjega roba prevlek. Dobil so fino mikrostrukturo in homogeno disperzijo ojačitvene faze TiB po celotnem preseku prevleke na vzorcih izdelanih z močjo laserja 3,0 kW. Mikrotrdota prevlek, izdelanih z razmerjem 90 % Ti in 10 % B prahu, je bila več kot 2-krat večja od podlage iz zlitine Ti-6Al-4V. Maksimalno povprečno trdoto prevleke 792,2 HV so dosegli pri moči laserja 3,0 kW. Mikrostrukture in lastnosti prevlek so se spreminjale s spreminjanjem moči (energije) laserskega snopa. Avtorji opisujejo vpliv skeniranja z laserjem različne moči na nastalo mikrostrukturo izdelanih kompozitnih prevlek.

Ključne besede: kompozitne prevleke, izdelava z laserskim pretaljevanjem, zlitina Ti-6Al-4V, skeniranje z močnim laserskim snopom, razvoj mikrostrukture

## 1 INTRODUCTION

Titanium alloys are known as “space metals” because of their excellent high-temperature performance,<sup>1-4</sup> corrosion resistance and comprehensive mechanical properties, which makes them popular in application fields with high requirements for workpiece surface, such as aerospace and other fields.<sup>5-8</sup> Due to the poor wear resistance and oxidation resistance, the safety and reliability of the structure are great influenced by titanium alloys, which limits its application in the industrial field as an important structural material. In order to improve the wear resistance of titanium alloys, laser cladding is often used as a surface-modification technology. The cladding material

is applied on the surface of the substrate to form a surface-cladding layer, thus increasing the wear resistance.<sup>9</sup> In order to prepare high-quality *in-situ* reinforced composite coatings, TiB, TiC,<sup>10</sup> VC and SiC<sup>11</sup> were compared. Because of its good mechanical properties and stable thermal expansion, TiB has a modulus of elasticity of 550 GPa, a coefficient of thermal expansion of  $8.6 \times 10^{-6} \text{ K}^{-1}$  and a density of  $4.51 \text{ g/cm}^3$ ,<sup>12</sup> so TiB is the most ideal reinforcement.<sup>13,14</sup> Laser-cladding surface-modification technology can improve the surface properties of titanium alloys on the basis of saving materials and reducing costs, which makes titanium alloys widely used. In previous studies, multifarious pre-placed powder systems of titanium-alloy coatings were proposed, such as Ti-B<sub>4</sub>C,<sup>15</sup> Ti-TiB<sub>2</sub>,<sup>16,17</sup> Ti-TiC,<sup>18</sup> but the investigations on titanium alloys coating with pre-placed

\*Corresponding author's e-mail:  
zhangyoufeng@sues.edu.cn (Youfeng Zhang)

Ti-B powders fabricated by YAG laser system were limited.<sup>19,20</sup> In this paper, the *in situ* TiB/Ti metal-matrix composite coatings in the presence of pre-placed Ti-B powders were fabricated by laser cladding with different laser scanning powers. The phase composition, microstructure evolution, hardness and friction and wear properties of the TiB/Ti composite coatings fabricated at different laser powers were studied.

## 2 EXPERIMENTAL PART

The nominal composition of the Ti-6Al-4V alloy in w/% was Al, 6.5; V, 4.26; Fe, 0.22; N, 0.03; C, 0.07; O, 0.14; and the balance, Ti. The cylindrical specimens of Ti-6Al-4V alloy were cut to  $\phi 50$  mm  $\times$  10 mm. The raw materials were mixed powders of 90 w/% Ti and 10 w/% B. The purity of the Ti powder and B powder were 99.2 % and 99.9 %, respectively. The weighed powder was poured into a ball mill according to the measurement ratio, and the mixed powder was obtained after dry mixing with an agate ball for 2 hours. Before cladding, the oil stain and surface contamination were removed to improve the bonding effect between the coating and the substrate. The mixed powder with the thickness of 0.4 mm is laid on the surface of the titanium alloy substrate. The laser-cladding process was performed by an IPG-YLS-5000W fiber laser with output power of 2.5 kW, 3.0 kW and 3.5 kW, a scanning speed of 5 mm/s, a spot diameter of 5.0 mm and a laser wavelength of  $(1075 \pm 5)$  nm to make a single-track cladding layer. The energy-distribution mode of the laser is Gaussian. The laser processing parameters of the samples are given in **Table 1**.

**Table 1:** Powder composition and laser parameters of the samples

Powders	Laser power / (kW)	Scanning speed / (mm/s)
90 % Ti + 10 % B	2.5	5
90 % Ti + 10 % B	3.0	5
90 % Ti + 10 % B	3.5	5

Samples of the laser-cladding coatings were cut, ground and then polished. The cross-sections of the samples were etched in a solution of HF: HNO<sub>3</sub> (at the ratio of 1:2). The phase structures were measured using X-ray diffractometry (XRD) with *Cu-K $\alpha$*  radiation (X'Pert PRO PANalytical). Microstructures and chemical compositions of the cladding coatings were characterised using scanning electron microscopy (SEM, Hitachi S-3400N) combined with energy-dispersive spectrometry (EDS). HXD-1000 tester was used to test the microhardness distribution on the cross section, the load was 500g, and the dwell time was 15 s. The friction-and-wear test was carried out by HT-600 friction-and-wear testing machine. The counterpart discs were made of annealed 45# carbon steel, the roughness surface was polished with 400# SiC grit paper prior to the wear tests. The applied

load was 50 N. The sliding speed was kept constant is 100 min<sup>-1</sup> and held for 1 h. The weight loss during the wear test was measured using an electronic balance FA2004 with a resolution of  $\pm 0.1$  mg.

## 3 RESULTS AND DISCUSSION

**Figure 1** shows the XRD patterns of the composite coatings under different laser powers. It can be seen that the composite coating is composed of  $\alpha$ -Ti and TiB phases. The pre-placed powders in the coating and the substrate absorb a lot of heat energy and melt instantly to form the molten pool at high temperature when the high-energy laser beam hits the surface of the mixed powders. The Ti and B elements in the pre-placed coating *in situ* reacted at high temperature and formed TiB. TiB is a kind of ceramic reinforcing phase with a high hardness, good wear resistance and corrosion resistance, which is beneficial to enhance the mechanical properties of a composite coating. The phase structure of the composite coating was not greatly affected by the different laser powers according to comparing the XRD patterns of the composite coating fabricated by different powers of 2.5 kW, 3.0 kW and 3.5 kW.

**Figure 2** shows the SEM micrographs of the cross-section of the composite coatings fabricated under different laser powers. It can be seen that the composite coating presents the morphology of a crescent after laser cladding because the laser was operated in Gaussian mode, showing that the laser energy density of the center area is higher than that of both sides areas. The irradiation energy of the laser beam of center is higher than that of the edges when the laser beam hits on the pre-placed coating surface, forming a temperature gradient in the horizontal direction and the surface tension gradient. The heat energy is transferred to the Ti alloy substrate by heat conduction, the substrate in the center area melts first due to the high energy of the laser beam and then the

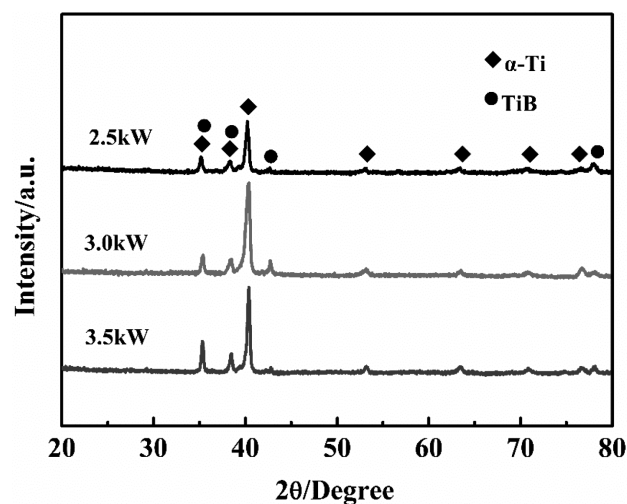


**Figure 1:** XRD patterns of the cladding composite coatings with different laser powers

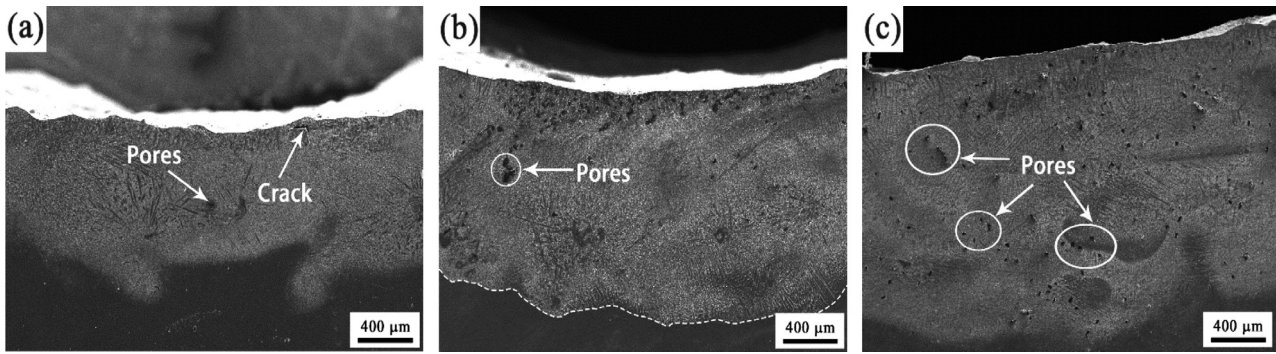


**Figure 2:** SEM micrographs of the cross-sections of cladding composite coatings: a) 2.5 kW, b) 3.0 kW and c) 3.5 kW

molten pool rapidly cooled, which led to the morphology of crescent occurred .

It can be seen in **Figure 2a** that the surface of the composite coating is flat and formed well with a thickness of 0.8–1.1 mm, and there is a clear bonding profile between the composite coating and the substrate at the laser power is 2.5 kW, indicating that they are metallurgical bonding well. However, there are a small amounts of pores in the middle and a micro-crack on the top of the cladding coating. **Figure 2b** shows there is an obvious white bonding band between the composite coating and the substrate at the laser power is 3.0 kW, which indicates that the metallurgical bonding is good. The surface of the composite cladding coating is flat and no cracks were observed, but pores exist. Most of the pores are distributed in the top and middle of the composite coating, and the thickness of the coating is about 1.1–1.3 mm. The gas in the molten pool is removed from the bottom to the top along with the convection of liquid metal during laser cladding process and the top of the molten pool contacts with the outside cold air first, resulting in that the bubbles in the top and middle of the molten pool cannot be removed in time, forming pores after cooling subsequently. As shown in **Figure 2c**, the composite coating formed well with the substrate by means of metallurgical bonding, but a large number of pores are scattered in the coating, and the coating thickness is about 1.1–1.8 mm at the laser power is 3.5 kW.

Comparing the morphologies of coatings fabricated by different laser powers in **Figure 2**, the thickness of

the composite coating increases gradually with the increase of the laser scanning power. This is because a part of the substrate will also be melted and enter the molten pool from the bottom of the molten pool with the convection of the liquid metal in the laser cladding process. Therefore, the laser energy density per unit area increases and the substrate melts more, resulting in the thickness of the composite coating becoming larger after cooling with the increase of the laser power. The microstructure of coating fabricated by laser power of 3.5 kW is the worst because the laser energy density is too high and the substrate melts more.

The micrographs of the top of the composite coatings obtained at different laser powers are shown in **Figure 3**. It can be seen that the composite coating is mainly composed of both black rod-like and a small amount of white needle-like phase when the laser power is 2.5 kW. The composite coating is mainly composed of black fishbone-like and white needle-like when the laser power is 3.0 kW. The former grows vertically, and the latter is evenly distributed in the coating. Compared with the coating prepared by 2.5 kW laser power, the number of white needle-like particles increased and the size decreased significantly in the coating prepared by a laser power of 3.0 kW. A large number of black fishbone-like are distributed in the composite coating and some white needle-like particles are filled in it when the laser power is 3.5 kW. Comparing the microstructure of the three samples, it shows that the structure of the coating fabricated by laser power of 3.0 kW is more uniform than

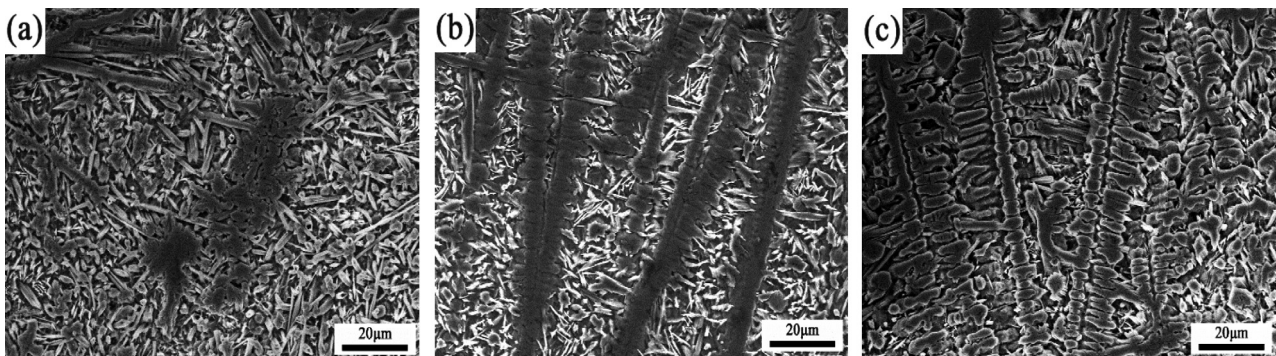


**Figure 3:** SEM micrographs of the top of the cladding composite coatings: a) 2.5 kW, b) 3.0 kW and c) 3.5 kW

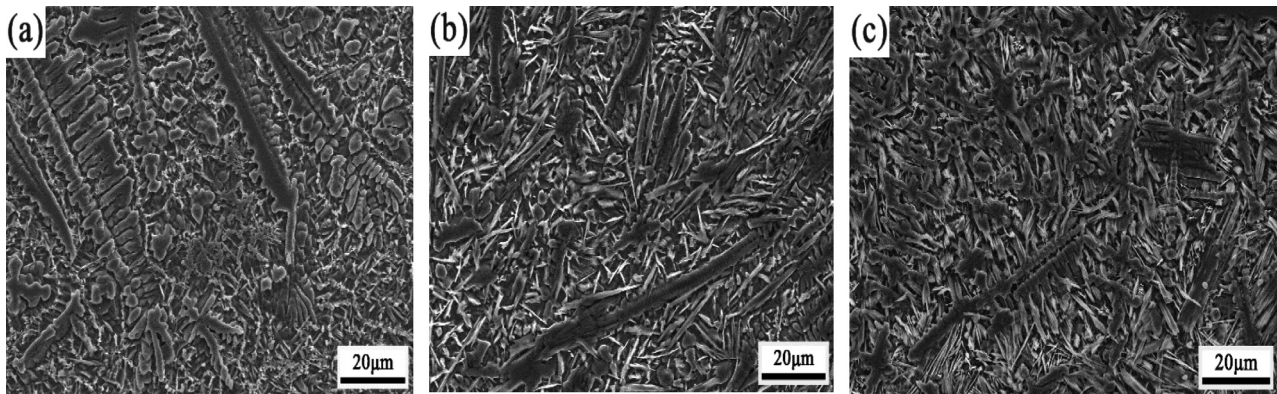


**Figure 4:** SEM micrographs of the middle of the cladding composite coatings: a) 2.5 kW, b) 3.0 kW and c) 3.5 kW

other samples fabricated by powers of 2.5 kW and 3.5 kW. The number of white needle-like phases exist and refine in the composite coating fabricated by a power of 3.0 kW.

**Figure 4** shows the SEM micrographs of the middle part of the laser cladding composite coatings with different laser powers. A large number of large-scale fishbone-like grains appear in the middle of the composite coating when the laser power is 2.5 kW. The number of fishbone-like grains is obviously reduced and is refined when the laser power is 3.0 kW and 3.5 kW, because of the energy absorbed increased by molten pool with the increase of laser power, which led to more cooling time and refined grains.

**Figure 5** shows the SEM micrographs of the bonding area of the composite coatings with different laser powers. The boundary of the bonding area of the composite coating and the substrate is clearly observed. It is straight in the coatings fabricated by a laser power of 2.5 kW and 3.5 kW and chaotic in coating of 3.0 kW. The grain grows and diffuses to the interior of the substrate in the composite coatings because the cooling effect of the Ti alloy substrate. This was attributed to the direction of the grain's growth, depending on the direction of the heat transfer in the high-temperature molten pool. Therefore, there is not enough time for the grains growing in the bonding zone, and microstructure of the bonding zone is finer than that of the other regions. Therefore, the metal-

lurgical bonding of the coating and substrate fabricated at 3.0 kW is well than other samples in the bottom of laser cladding coatings.

The microhardness of the cross-sections of the TiB/Ti composite coatings prepared by different laser powers are given in **Figure 6**. It can be seen that the microhardness of the composite coating decreases along the direction of distance from the surface, and then gradually stabilizes at about 350 HV. The average microhardnesses of the composite coatings are 688.02 HV, 792.17 HV and 776.87 HV, respectively. The average microhardness of the composite coating is higher than other samples when the laser power is 3.0 kW. It is consistent with the above microstructure. The microhardness of the composite coatings by laser cladding is higher than that of the titanium alloy, the maximum hardness of the synthesized TiB/Ti composites coating is 2.3-fold of the Ti-6Al-4V titanium alloy substrate. The specimen fabricated with laser power of 3.0 kW exhibited the highest hardness compared to the specimens of the others by 2.5 kW and 3.5 kW. In the composite coating, TiB has the highest hardness and the Ti substrate has the lowest hardness. The increased hardness is attributed to the reinforcement in composite coating. In this process, the composite coating with smooth surface, fined microstructure and higher microhardness can be obtained when laser power is 3.0 kW. Generally speaking, the microhardness of coatings effects the wear resistance of materials, so the higher the

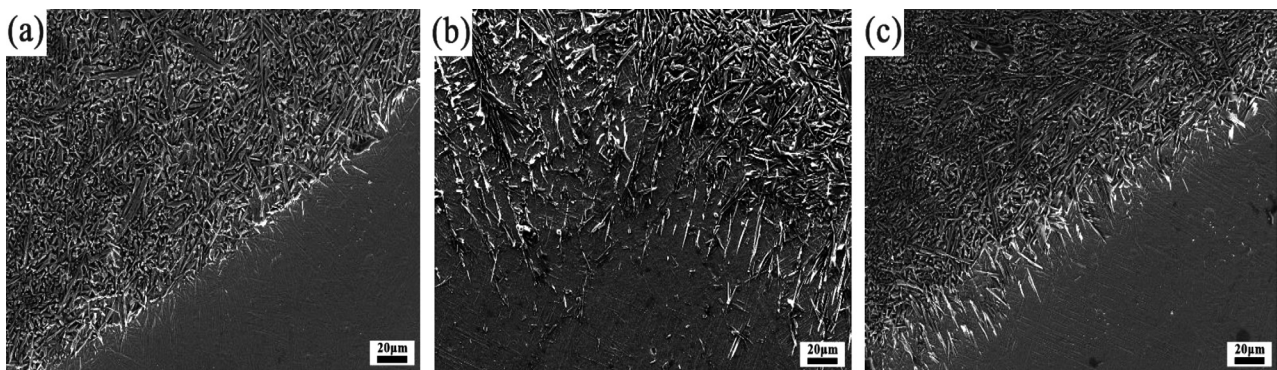


**Figure 5:** SEM micrographs of the bonding zone of the cladding composite coatings: a) 2.5 kW, b) 3.0 kW and c) 3.5 kW

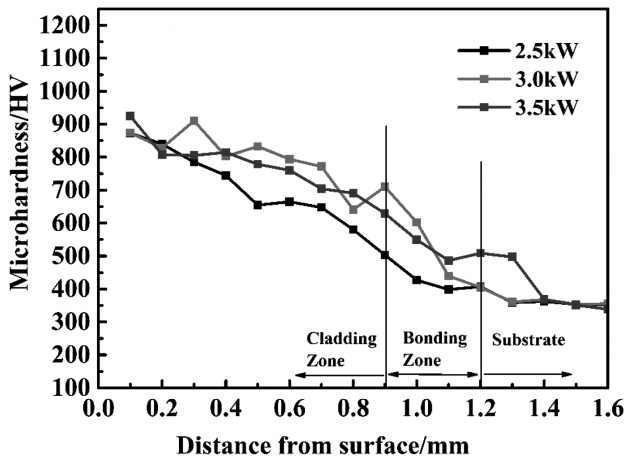


Figure 6: Microhardness of the laser cladding composite coatings

microhardness is beneficial for application as a wear-resistant material.

In order to investigate the friction and wear properties, the sample fabricated by laser power of 3.0 kW was chosen for wear test and compared with the substrate of

Ti alloy. The friction coefficient of the tested coating and Ti alloy substrate as a function of time were measured and the results are shown in Figure 7. The classical mechanics sliding friction formula is as follows:

$$f = \mu \cdot F_N \quad (1)$$

where  $f$  is the sliding friction (N),  $\mu$  is the friction coefficient and  $F_N$  is the positive pressure (N). Under the condition of ensuring that the positive pressure remains unchanged, the smaller the friction coefficient, the smaller the friction, and the stronger the friction resistance.

As shown in Figure 7, the friction coefficient of the substrate is obviously higher than that of the cladding composite coating fabricated by laser power of 3.0 kW, and the average friction coefficient of substrate and coating are about 0.84 and 0.70, respectively. Table 2 shows the result of the wear weight loss ratio tests made on coating fabricated with laser power of 3.0 kW and substrate. It can be seen that the wear weight loss ratio of the substrate is larger than that of the coating. The laser cladding surface exhibited good wear resistance and a

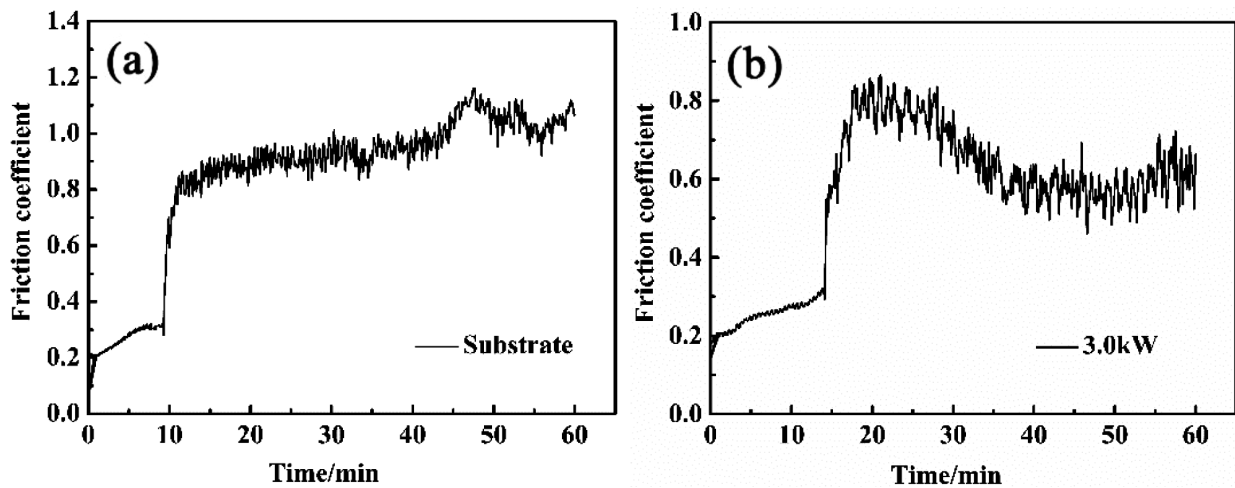


Figure 7: Instantaneous friction curve of samples: a) substrate and b) coating

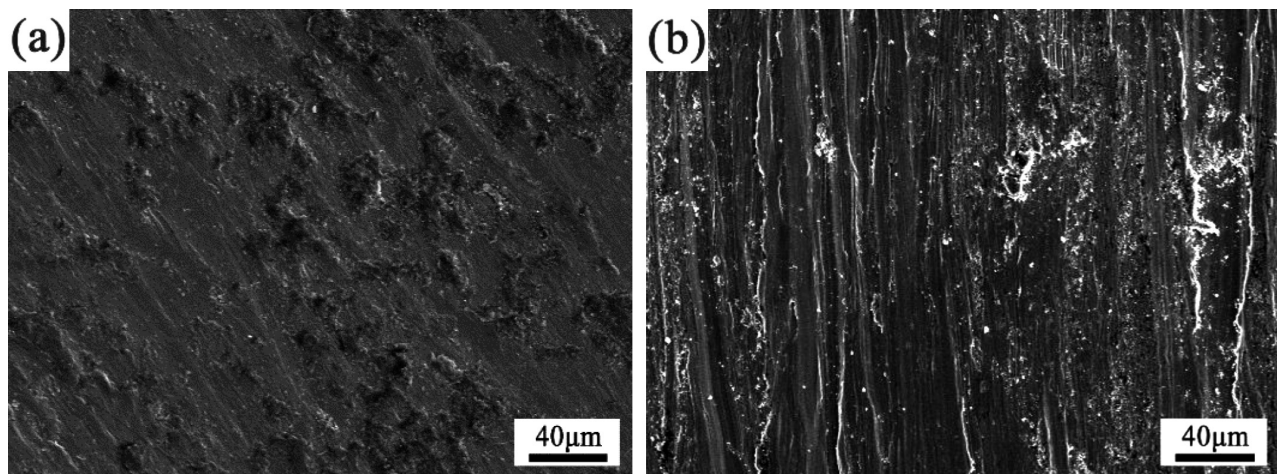


Figure 8: SEM micrographs of the surface wear marks of substrate and cladding coating: a) substrate and b) coating

lower wear weight loss ratio. In general, the wear resistance is proportional to the hardness of coatings; the presence of the TiB increases the hardness of composite coating. Both the friction coefficient and wear weight loss ratio of the composite coating decreased.

**Table 2:** Wear weight loss ratio of substrate and cladding coating

Samples	Wear weight loss ratio
Substrate	0.079 %
Coating	0.072 %

**Figure 8** shows the SEM surface morphologies of the substrate and coating fabricated with laser power of 3.0 kW after the wear process. It can be observed that there are many deep fits obviously on the wear surface of the titanium alloy substrate with a large scale of peeling. On the wear surface of the cladding composite coating, there are some obvious furrows and bumps, and the furrows are small and uniform. The surface of the cladding layers with shallow wear traces is much smoother than that of substrate and there are granular grindings in the abrasive surface, which are scratched by rubbing the surface of the cladding material during the rubbing process.

## 4 CONCLUSIONS

In summary, laser cladding surface modification was applied to a Ti-6Al-4V alloy using mixed powders of 90 w/% Ti and 10 w/% B. The effect of different laser cladding powers on the phase composition, microstructure evaluation and wear properties of the cladding coatings was investigated. The coatings comprised black fishbone-shaped  $\alpha$ -Ti dendrites and white needle-like TiB particles when a laser scanning speed of 5 mm/s and a laser power of 2.5 kW, 3.0 kW and 3.5 kW were used. The cladding coating and the substrate combined metallurgically after the laser-cladding process, and no obvious cracks found in the cladding coating fabricated at laser power of 3.0 kW. The black fishbone-shaped  $\alpha$ -Ti dendrites exist more in the top of coatings, the white needle-like TiB particles structure gradually increased in the middle of coatings and the micro-needle particles mainly exist in the bottom of coatings. The TiB reinforcement dispersed homogeneously in the composite coatings fabricated with laser power of 3.0 kW and it is more uniform than other samples fabricated by 2.5 kW and 3.5 kW. The microhardness of the cladding coatings fabricated with different powders was over two-times greater than that of the Ti-6Al-4V titanium alloy substrate and achieved a maximum average of 792.17 HV when laser power was 3.0 kW. The wear resistance of the composite coatings fabricated by laser power of 3.0 kW was improved obviously. The microstructures and mechanical properties of the coatings can be controlled by adjusting the laser cladding power. High-performance *in situ* synthesized TiB/Ti composite coating can be obtained by the laser cladding process.

## Acknowledgment

This work was supported by the Nature Science Foundation of China (No. 11604204).

## 5 REFERENCES

- B. F. He, D. Y. Ma, F. Ma, K. W. Xu, Microstructures and wear properties of TiC coating produced by laser cladding on Ti-6Al-4V with TiC and carbon nanotube mixed powders, *Ferroelectrics*, 547 (2019) 1, 217–225, doi:10.1080/00150193.2019.1592502
- Y. J. Zhai, X. B. Liu, S. J. Qiao, M. D. Wang, X. L. Lu, Y. G. Wang, Y. Chen, L. X. Ying, Characteristics of laser clad  $\alpha$ -Ti/TiC + (Ti,W) $C_{1-x}$ /Ti $_2$ SC + TiS composite coatings on TA2 titanium alloy, *Optics and Laser Technology*, 89 (2017), 97–107, doi:10.1016/j.optlastec.2016.09.044
- I. Sen, S. Tamirisakandala, D. B. Miracle, U. Ramamurty, Microstructural effects on the mechanical behavior of B-modified Ti-6Al-4V alloys, *Acta Materialia*, 55 (2007) 15, 4983–4993, doi:10.1016/j.actamat.2007.05.009
- J. Li, Z. S. Yu, H. P. Wang, Wear behaviors of an (TiB+TiC)/Ti composite coating fabricated on Ti6Al4V by laser cladding, *Thin Solid Films*, 519 (2011) 15, 4804–4808, doi:10.1016/j.tsf.2011.01.034
- R. L. Sun, D. Z. Yang, L. X. Guo, S. L. Dong, Laser cladding of Ti-6Al-4V alloy with TiC and TiC+NiCrBSi powders, *Surface and Coatings Technology*, 135 (2001) 2-3, 307–312, doi:10.1016/S0257-8972(00)01082-3
- Y. L. Yang, D. Zhang, W. Yan, Y. R. Zheng, Microstructure and wear properties of TiCN/Ti coatings on titanium alloy by laser cladding, *Optics and Lasers in Engineering*, 48 (2010) 1, 119–124, doi:10.1016/j.optlaseng.2009.08.003
- Y. S. Tian, C. Z. Chen, S. T. Li, Q. H. Huo, Research progress on laser surface modification of titanium alloys, *Applied Surface Science*, 242 (2005) 1–2, 177–184, doi:10.1016/j.apsusc.2004.08.011
- B. G. Guo, J. S. Zhou, S. T. Zhang, H. D. Zhou, Y. P. Pu, J. M. Chen, Microstructure and tribological properties of in situ synthesized TiN/Ti3Al intermetallic matrix composite coatings on titanium by laser cladding and laser nitriding, *Materials Science and Engineering A-Structural Materials Properties Microstructure and Processing*, 480 (2008), 404–410, doi:10.1016/j.msea.2007.07.010
- O. F. Ochonogor, C. Meacock, M. Abdulwahab, S. Pityana, A. P. I. Popoola, Effects of Ti and TiC ceramic powder on laser-cladded Ti-6Al-4V in situ intermetallic composite, *Applied Surface Science*, 263 (2012) 15, 591–596, doi:10.1016/j.apsusc.2012.09.114
- Y. H. Lv, J. Li, Y. F. Tao, L. F. Hu, Oxidation behaviors of the TiNi/Ti2Ni matrix composite coatings with different contents of TaC addition fabricated on Ti6Al4V by laser cladding, *Journal of Alloys and Compounds*, 679 (2016) 15, 202–212, doi:10.1016/j.jallcom.2016.04.037
- M. Das, S. Bysakh, D. Basu, T. S. Sampath Kumar, V. Krishna, Balla S. Bose, A. Bandyopadhyay, Microstructure, mechanical and wear properties of laser processed SiC particle reinforced coatings on titanium, *Surface and Coatings Technology*, 205 (2011) 19, 4366–4373, doi:10.1016/j.surfcoat.2011.03.027
- Z. Fan, A. P. Miodownik, L. Chandrasekaran, M. Ward-Close, The Young's moduli of in situ Ti/TiB composites obtained by rapid solidification processing, *Journal of Materials Science*, 29 (1994), 1127–1134, doi:10.1007/BF00351442
- L. F. Cai, Y. Z. Zhang, and L. K. Shi, Microstructure and formation mechanism of titanium matrix composites coatings on Ti-6Al-4V by laser cladding, *Rare Metals*, 26 (2007) 5, 342–346, doi:10.1016/S1001-0521(07)60226-5
- F. Wang, J. Mei, X. H. Wu, Direct laser fabrication of Ti6Al4V/TiB, *Journal of Materials Processing Technology*, 195 (2008) 1–3, 321–326, doi:10.1016/j.jmatprotec.2007.05.024
- D. R. Ni, L. Geng, J. Zhang, Z. Z. Zheng, Effect of B $_4$ C particle size on microstructure of in situ titanium matrix composites prepared by

- reactive processing of Ti–B<sub>4</sub>C system, *Scripta Materialia*, 55 (2006) 5, 429–432, doi:10.1016/j.scriptamat.2006.05.024
- <sup>16</sup> P. Chandrasekar, V. Balusamy, K. S. Ravi Chandran, H. Kumar, Laser surface hardening of titanium–titanium boride (Ti–TiB) metal matrix composite, *Scripta Materialia*, 56 (2007) 7, 641–644, doi:10.1016/j.scriptamat.2006.11.035
- <sup>17</sup> V. Ocelik, D. Matthews, J. Th. M. De Hosson, Sliding wear resistance of metal matrix composite layers prepared by high power laser, *Surface and Coatings Technology*, 197 (2005) 2–3, 303–315, doi:10.1016/j.surfcoat.2004.09.003
- <sup>18</sup> J. C. Oh, D. K. Choo, S. Lee, Microstructural modification and hardness improvement of titanium-base surface-alloyed materials fabricated by high-energy electron beam irradiation, *Surface and Coatings Technology*, 127 (2000) 1, 76–85, doi:10.1016/S0257-8972(99)00664-7
- <sup>19</sup> Y. S. Tian, Q. Y. Zhang, D. Y. Wang, C. Z. Chen, Analysis of the Growth Morphology of TiB and the Microstructure Refinement of the Coatings Fabricated on Ti-6Al-4V by Laser Boronizing, *Crystal Growth & Design*, 8 (2008) 2, 700–703, doi:10.1021/cg0608099
- <sup>20</sup> R. Banerjee, A. Genc, P.C. Collins, H. L. Fraser, Comparison of microstructural evolution in laser-deposited and arc-melted In-Situ Ti–TiB, *Metallurgical and Materials Transactions A-Physical Metallurgy and Materials Science*, 35 (2004), 2143–2152, doi:10.1007/s11661-004-0162-0